Applied Catalysis B: Environmental 111–112 (2012) 461–466

Contents lists available at SciVerse ScienceDirect

Applied Catalysis B: Environmental

journal homepage: www.elsevier.com/locate/apcatb

Controlled synthesis of highly active mesoporous Co_3O_4 polycrystals for low temperature CO oxidation

Yingjun Feng[a], Liang Li[a,*], Shufan Niu[a], Yan Qu[a], Qian Zhang[a], Yongsheng Li[a], Wenru Zhao[a], Hua Li[a], Jianlin Shi[a,b,**]

[a] Laboratory for Advanced Functional Materials, School of Materials Science and Engineering, East China University of Science and Technology, Shanghai 200237, China
[b] State Key Laboratory of High Performance Ceramic and Superfine Microstructure, Shanghai Institute of Ceramics, Chinese Academy of Sciences, Shanghai 200050, China

ARTICLE INFO

Article history:
Received 7 July 2011
Received in revised form 17 October 2011
Accepted 24 October 2011
Available online 4 November 2011

Keywords:
Cobalt oxide
Catalyst
Mesoporous materials
CO oxidation

ABSTRACT

Polycrystalline mesoporous Co_3O_4 has been successfully fabricated using a simple but efficient controlled thermal decomposition approach and their catalytic activities for low temperature CO oxidation were evaluated. In such a synthesis, micrometer-sized polyhedral cobalt oxalate crystals were first prepared and used as precursor. Mesoporosity was then generated via the pyrolysis of the cobalt oxalate precursor and the resultant nano-sized Co_3O_4 crystallites connected together to form mesoporous structure within the original micrometer-sized particles. The as-prepared material by calcination at 300 °C at a heating rate of 0.5 °C/min possessed high surface area and showed extraordinarily high catalytic activity for low temperature CO oxidation, the full CO conversion can be achieved at as low as −70 °C.

1. Introduction

Since the discovery of active nano-sized gold catalysts attached on metal oxide particles by Haruta et al. [1,2], low temperature catalytic oxidation of CO has been studied extensively due to its great importance for both practical applications and fundamental researches. Gold nanoparticles deposited on reducible semiconductor metal oxides, hydroxides of alkaline earth metals, and amorphous ZrO_2 were highly active for CO oxidation at ambient and sub-ambient temperatures [3–8]. However, the scarcity and high cost of noble metals stimulated extensive searching for other low cost catalysts. Considerable efforts have been devoted to the development of CO oxidation catalysts based on transition metal oxides, and some base oxides such as Co_3O_4, NiO, and mixtures of MnO_2 and CuO (called Hopcalite) were found to be also active at low temperature for CO oxidation [9–14]. In particular, among these transition metal oxides, Co_3O_4 nanostructure has received increasing interest as promising CO oxidation catalysts of high low-temperature catalytic activity [11–16].

Dependent on the preparation routes for the materials and the reaction conditions, Co_3O_4 showed varied activities for CO oxidation. Xu and co-works prepared Co_3O_4 nanosheets by an *in situ* dealloying method combined with an oxidation process, the resultent catalysts had a full CO conversion at around 110 °C [12]. Through a nanocasting process, Tűysűz et al. synthesized mesoporous Co_3O_4 of excellent CO oxidation activity at ambient temperature [13]. The light-off temperature of CO decreased with the increasing surface area of ordered mesoporous Co_3O_4. Recently, Xie et al. reported the preparation of Co_3O_4 nanorods by a morphology-controlled method using ethylene glycol as an organic solvent followed by calcining the cobalt hydroxide carbonate precursor at 450 °C, and found that the resulting materials were steadily active for CO oxidation at as low as −77 °C [14]. This report presented that Co_3O_4 was active for CO oxidation below room temperature only when specific crystalline planes were exposed at the surface. In summary, the performance of Co_3O_4 in catalysis could be optimized by increasing surface area, decreasing particle size distribution and preferentially exposing more active lattice planes.

In the present work, we report a simple but efficient approach to synthesize mesoporous Co_3O_4 polycrystalline catalyst by a controlled thermal decomposition of cobalt oxalate crystals. In such a synthesis, micrometer-sized polyhedral cobalt oxalate crystals was first prepared, and then mesopore structure was generated via the pyrolysis of the precursors, the obtained materials inherited original polyhedral morphology and possessed extensive mesoporous structure among nano-sized Co_3O_4 crystallites. The as-prepared materials possessed high surface area and showed excellent catalytic activity for low temperature CO oxidation.

* Corresponding author. Tel.: +86 21 64250740; fax: +86 21 64250740.
** Corresponding author at: State Key Laboratory of High Performance Ceramic and Superfine Microstructure, Shanghai Institute of Ceramics, Chinese Academy of Sciences, Shanghai 200050, China.
E-mail addresses: liliang@ecust.edu.cn (L. Li), jlshi@sunm.shcnc.ac.cn (J. Shi).

0926-3373/$ – see front matter © 2011 Elsevier B.V. All rights reserved.
doi:10.1016/j.apcatb.2011.10.035

2. Experimental

2.1. Synthesis of CoC_2O_4 crystals

In a typical synthesis, 0.009 mol $CoCl_3{\cdot}6H_2O$ (Fluka, 99% ACS reagent) and 0.004 mol Sodium dioctylsulfosuccinate (AOT surfactant) (Sigma Aldrich, 96% ACS reagent) were dissolved in 200 ml deionized water at 80 °C and stired for 4 h, then 20 ml oxalic acid solution (containing 0.01 mol oxalic acid and little phosphoric acid) was slowly dropped and vigorously stirred for 15 min. The resulting mixture was quickly cooled down in ice-water and a large amount of white precipitate was obtained. After filtration and washing with deionized water, the precipitate was dried at 60 °C for 6 h.

2.2. Synthesis of mesoporous cobalt oxide polycrystal

A series of mesoporous cobalt oxides were obtained by calcining the precursor $CoC_2O_4{\cdot}2H_2O$ at the temperature from 250 °C to 400 °C for 4 h. The heating rate during calcinations were fixeded at 0.5 °C·min^{-1}.

2.3. Characterization

X-ray diffraction (XRD) data were collected using a Bruk D8 Focus powder diffractometer with graphite monochromatized Cu Kα radiation (λ = 0.15405 nm). N_2 adsorption and desorption isotherms were measured at 77 K on a micromeritics ASAP 2020 system. The specific surface area and the pore size distribution were calculated using the BET and Barrett–Joyner–Halenda (BJH) methods, respectively. Transmission electron microscopy (TEM) observations were performed on a field emission JEM-3000F (JEOL) electron microscope operated at 300 kV equipped with a Gatan-666 electron energy loss spectrometer and energy dispersive X-ray spectrometer. XPS (X-ray photoelectron spectroscopy) signals were collected on a VG Micro MK II instrument using monochromatic Al Kα X-ray at 1486.6 eV operated at 200 W. All the elemental binding energies were referenced to the C (1s) line situated at 284.6 eV. Thermogravimetric analysis (TG-DTA) were carried out at a heating rate of 10 °C/min form ambient temperature to 700 °C with an air flow rate of 20 ml min^{-1}. H_2 temperature-programmed reduction (H_2-TPR) analysis was performed by using an automatic chemsorpion analyzer (TP5080) equipped with a TCD dictater. For each analysis, approximately 20 mg sample was treated with a 25 mL min^{-1} stream of 5 vol% H_2 in Argon from ambient temperature to 600 °C at heating rate of 10 °C/min.

2.4. CO oxidation test

The catalytic tests for CO oxidation was carried out in fixed-bed quartz reactor (i.d. = 6 mm) containing 100 mg of catalyst samples without any pretrement. A standed reaction gas containing 1.0 vol% CO, 4.0 vol% O_2 and 95 vol% N_2, and a high-purity N_2 (99.99%) gas were dried first by zeolite and used as sources to form desired gas mixture. The feed gas at a flow rate of 100 ml min^{-1} was directly introduced into the reactor. After the steady operation for 10 min, the activity of catalyst was tested. The reaction temperature was controlled by using ethanol/liquid nitrogen mixture in a vacuum bottle below room temperature, by using warm water bath above room temperature. The conversion of CO was measured by online gas chromatograph.

3. Results and discussion

The cobalt oxalate crystalline precursor ($CoC_2O_4{\cdot}2H_2O$) was synthesized similar to the method reported by Yu et al. using sodium dioctylsulfosuccinate (AOT) surfactant as structure directing agent [17]. Mesoporous structured Co_3O_4 polycrystalline particles were obtained through a controlled thermal decomposition of cobalt oxalate. In general, the decomposition process has a strong effect on crystallite size and the texture of the product, in addition to the catalytic activity. In order to determine an appropriate pyrolysis temperature, the thermal behavior of $CoC_2O_4{\cdot}2H_2O$ sample was first investigated by TG–DTA analysis at a heating rate of 10 °C/min, as presented in Fig. 1. When calcined to 800 °C, the cobalt oxalate precursor lost 53.2% of its original weight in two steps. These weight losses were accompanied by an endotherm at about 160 °C and an exotherm at about 284 °C, suggesting the elimination of coordinated water and the combustion of the decomposition product of anhydrous cobalt oxalates, respectively. Cong et al. [18] reported that the decomposition temperature can be decreased to about 250 °C at a heating rate of 1 °C/min. Thus, cobalt oxalates crystalline precursor could be completely decomposed at the temperature at or above 250 °C for long enough time.

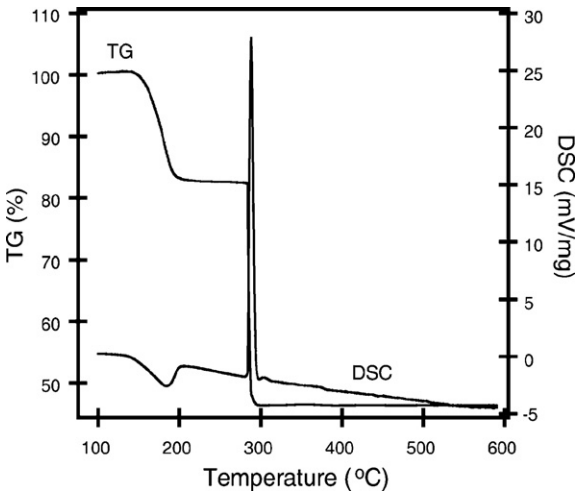

Fig. 1. TG and DSC curves for prepared cobalt oxalate hydrate.

After calcined at 250 °C or above for 4 h, the cobalt oxalate crystals were totally decomposed and converted to cobalt oxide. The decomposed products were labeled as C_1, C_2, C_3 and C_4, corresponding to the calcination temperatures of 250 °C, 300 °C, 350 °C and 400 °C, respectively. The X-ray diffraction (XRD) patterns of cobalt oxalate and its calcined products are shown in Fig. 2, which clearly indicates that the as-synthesized precipitate is the crystallized cobalt oxalate dihydrate. After calcination, the materials lost their original crystalline structure and turned into nano-sized spinel Co_3O_4 crystallites. The textural properties of the resulting cobalt oxides were further investigated by measuring adsorption–desorption isotherms of nitrogen at 77 K, as shown in Fig. 3. In all cases, the type IV isotherms suggest the mesoporous structures and the appearance of H3 hysteresis loops indicates the formation of slit-like meso-pores. These pores were generated from the decomposition and mass loss of cobalt oxalate hydrate crystals during pyrolysis. Thus, the specific surface area and pore volume of the resulting materials are highly dependent on calcination temperature and heating program. Over high temperature pyrolysis will induce the extensive growth of the cobalt oxide nanocrystals and the collapse of the pore network, resulting in much decreased specific surface area and pore volume. For cobalt oxide calcined at 250 °C, the specific surface area and pore volume are 207 m^2 g^{-1} and 0.4 cm^3 g^{-1}, respectively, but for that calcined at 400 °C, they decreased quickly down to 52 m^2 g^{-1} and 0.14 cm^3 g^{-1}, respectively.

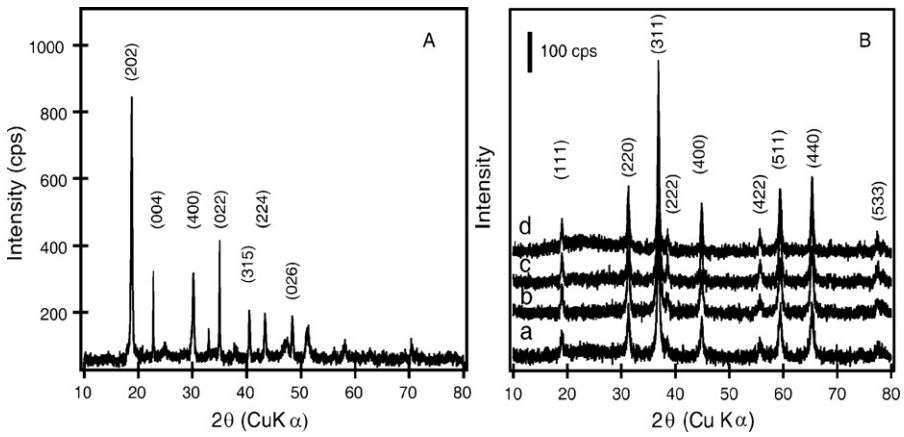

Fig. 2. (A) XRD patterns of $CoC_2O_4{\cdot}2H_2O$; (B) XRD patterns of cobalt oxides calcined at (a) 250 °C, (b) 300 °C, (c) 350 °C, (d) 400 °C.

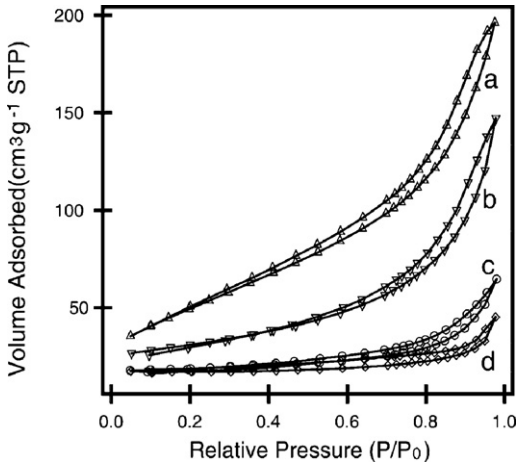

Fig. 3. N_2-adsorption–desorption isotherms of Co_3O_4 catalysts calcined at (a) 250 °C, (b) 300 °C, (c) 350 °C, (d) 400 °C.

Fig. 4 shows the SEM images of as-prepared cobalt oxalate dehydrate and decomposed mesoprous cobalt oxides at different temperatures. The well-crystallized oxalate precursors are mostly regular polyhedrons of several micrometers in size. This morphology was preserved even after calcination at 400 °C due to the very low heating rate. Compared with the image of as-prepared cobalt oxalate, the major difference in their SEM images, after calcination, is their surface roughness. Broad cracks and large pores can also be found spreading all over the particle surface. There is no significant difference among the SEM images calcined at different temperatures. The crystalline structures of the calcined samples were further characterized by TEM observations, as depicted in Fig. 5. The images prove that the materials possess mesoporous structure with the pore network inter-sectioned by the cobalt oxide nanocrystals. A slow heating rate of 0.5 °C/min was essential to gain this porous structure. Rapid heating of the sample could cause the remarkable shrinkage and disrupture of the polyhedron morphology due to the violent gas evolution of steam and carbon oxide. The TEM images also indicate that both the mesopore and nanocrystal sizes are uniform for the materials calcined at the given temperatures and increase at elevated heating temperature from 250 °C to 400 °C. These results correspond well with the N_2 adsorption–desorption isotherms discussed above.

FT-IR data shown in Fig. 6 demonstrate the chemical and structural changes of the materials described above. The as-prepared cobalt oxalate dehydrate showed a strong absorption band at 1627 cm^{-1} and two sharp bands 1437 cm^{-1} and 1327 cm^{-1}, which were attributable to asymmetric and symmetric stretching vibrations of $C_2O_4^{2-}$, respectively. After calcination, the signals at 1437 cm^{-1} and 1327 cm^{-1} disappeared indicating the complete

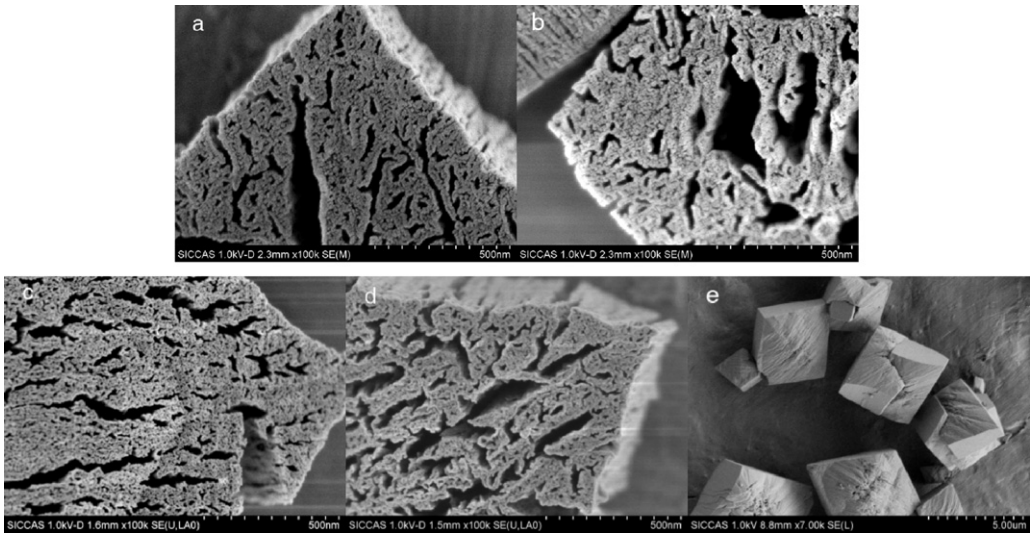

Fig. 4. SEM images of and Co_3O_4 catalysts calcined at (a) 250 °C, (b) 300 °C, (c) 350 °C, (d) 400 °C and SEM image of $CoC_2O_4{\cdot}2H_2O$ (e).

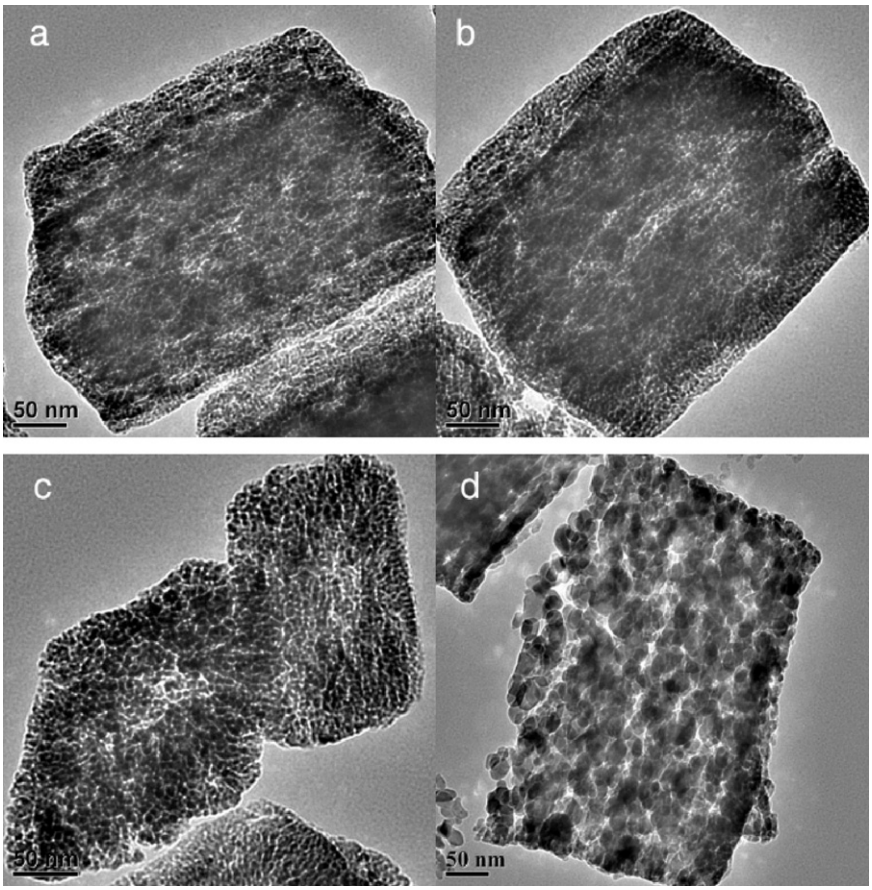

Fig. 5. TEM images of Co_3O_4 catalysts calcined at (a) 250 °C, (b) 300 °C, (c) 350 °C, (d) 400 °C.

decomposition of the $C_2O_4^{2-}$. Although there was still a weak absorption band near 1627 cm^{-1}, this can be ascribed to the bending vibrations of absorbed water molecules in the sample, as could also be proved by stretching vibration band at about 3400 cm^{-1}. Furthermore, two strong peaks at 665 cm^{-1} and 569 cm^{-1} evolved, which were attributable to Co–O stretching and bending vibrations mode of cobalt oxide, again indicating the decomposition of cobalt oxalate.

To gain further information on surface composition of the calcined samples, X-ray photoelectron spectroscopy (XPS) analysis was performed. The Co 2p XPS spectra of cobalt oxide are shown in Fig. 7A. The spectra show two main peaks at about 780 eV and 796 eV. Generally, Co_3O_4 have two types of cobalt ions, tetrahedral Co^{2+} and octahedral Co^{3+} contributing to 2p spectral profile, Paramagnetic Co(II) oxide has a strong shake-up satellite 6 eV above the Co $2p_{3/2}$, while normal diamagnetic cobalt(III) oxide usually does not [19]. The relatively sharp peak width, $2p_{1/2}$ to $2p_{3/2}$ separation of 16 eV and the very flat, weak satellite structure found in the high binding energy side of $2p_{3/2}$ and $2p_{l/2}$ transitions indicate the co-existence of Co(II) and Co(III) on the surface of the materials calcined at 300 °C. When calcined at relatively higher temperatures (350 °C and 400 °C), two main peaks shifted to lower binding energy side and the satellite almost disappeared, suggesting that only few high spin Co(II) cations occupied octahedral sites in the spinel lattice and that the majority of cobalt ions found on the surface octahedral sites were diamagnetic (low spin) Co(III). As to the catalyst prepared at 250 °C, the satellite became relative higher than that of 300 °C, indicating more surface Co^{2+} ions. The Co 2p XPS spectra also show that the intensity of Co single dropped with the annealing temperature. This can be attributed to the decreased Co content. Element analysis indicated that the Co content in the calcined samples is 73.4%, 72.2%, 71.5% and 71.4% for C1–C4, respectively. They are all somewhat nonstoichiometry. The XPS O 1 s spectra of the samples were also listed in Fig. 7B. They all consist of two components. The peak at around 529.6 eV is due to lattice O, while the peak at about 531.6 eV can be attributed to the low coordinated oxygen ions (chemisorbed oxygen) at the surface. The intensity of the XPS O 1 s peak is rising with the annealing temperature indicating the more surface oxygen content. This result consists well with the above Co XPS analysis.

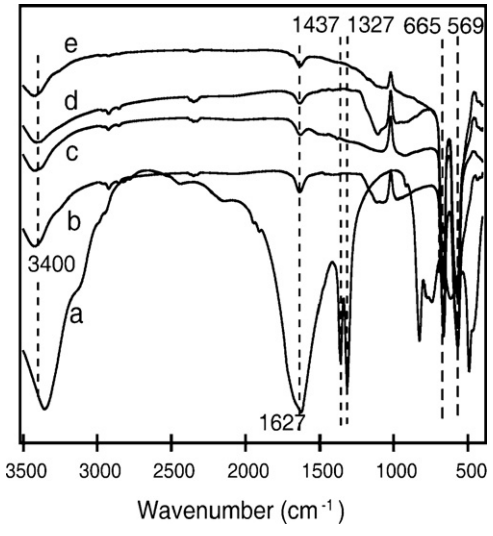

Fig. 6. FT-IR spectra of $CoC_2O_4{\cdot}2H_2O$ (a) and Co_3O_4 catalysts calcined at (b) 250 °C; (c) 300 °C, (d) 350 °C, (e) 400 °C.

H_2-TPR experiments were performed over catalysts prepared at different decomposition temperatures to investigate their

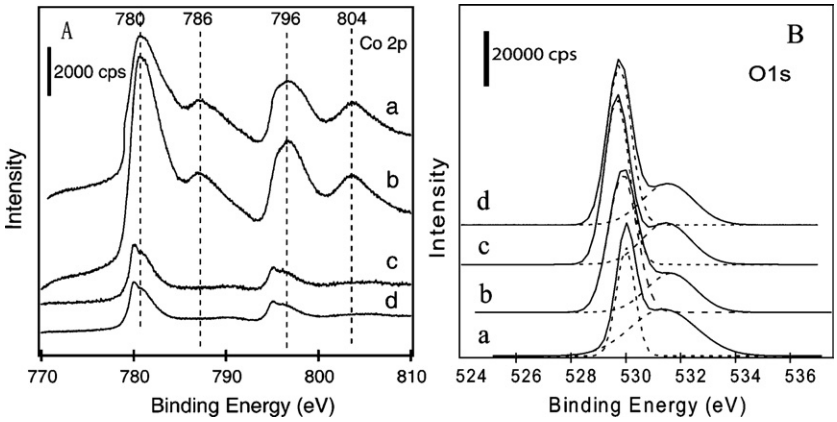

Fig. 7. (A and B) XPS spectra of Co_3O_4 catalysts calcined at (a) 250 °C, (b) 300 °C, (c) 350 °C, (d) 400 °C.

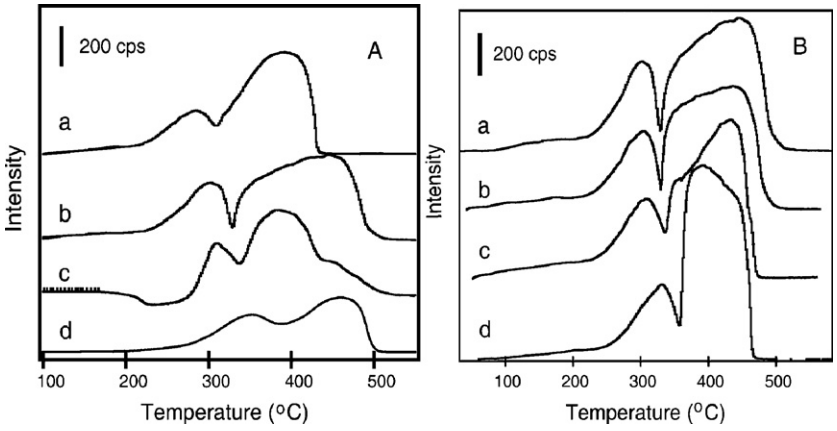

Fig. 8. (A) H_2-TPR profiles of the Co_3O_4 catalysts calcined at (a) 250 °C, (b) 300 °C, (c) 350 °C, (d) 400 °C. (B) H_2-TPR profiles of the Co_3O_4 catalysts calcined at 300 °C under different heating rates of (a) 0.5 °C/min, (b) 1 °C/min, (c) 2 °C/min, (d) 5 °C/min.

reduction behavior. The TPR profiles of these catalysts are shown in Fig. 8A. For all the catalysts, there are two well-defined reduction peaks in their profiles corresponding to the stepwise reduction of Co_3O_4 to metallic cobalt. According to the literatures [20,21], the first reduction peak centered at about 300 °C can be attributed to the reduction of Co_3O_4 to CoO, and the second in the region of 350–450 °C is due to the reduction of CoO to metallic cobalt. The corresponding chemical equations indicate that H_2 consumption in these two reduction steps should be 1:3 theoretically. In our experiment, the catalyst prepared at 250 °C showed the lowest reduction temperature but the ratio of hydrogen consumption in two reduction steps reached 1:4.5, indicating the excess Co^{2+} in the 250 °C-calcined materials. The result consists well with that of XPS analysis discussed above. Only the catalyst prepared at 300 °C has the ratio (1:3.1) close to 1:3. As to the catalyst prepared at higher temperatures, the reduction of Co^{3+} to Co^{2+} must occur more extensively. The effect of heating program on the oxidation properties was also investigated by H_2-TPR experiment, as shown in Fig. 8B. For the catalyst calcined at 300 °C, the relatively low reduction temperature of Co^{3+} to Co^{2+} and consequently the improved oxidation properties can be obtained at lower heating rates. The above results clearly indicate that preparation parameters of the catalysts can significantly affect the chemical properties of fabricated mesoporous cobalt oxide in addition to its pore structure and crystallite size.

The catalytic activities of the samples calcined at different temperatures are given in Fig. 9. As one can see, CO full conversion temperatures of the catalysts are all lower than −35 °C. Although the catalyst calcined at 250 °C (C1) has the largest surface area and the smallest particle size, its full conversion temperature was −40 °C probably due to its much higher Co^{2+} content. As for the catalysts prepared at 350 °C and 400 °C, the full conversion temperatures were about −50 °C and −35 °C, respectively, probably due to their much decreased surface area. In comparison, the catalyst obtained at 300 °C (C2) has a relatively higher catalytic activities, its full conversion reached −70 °C. This conversion temperature is highly comparable to that reported on the Co_3O_4 nanorods [14], in which the exposure of specific lattice planes was necessary for

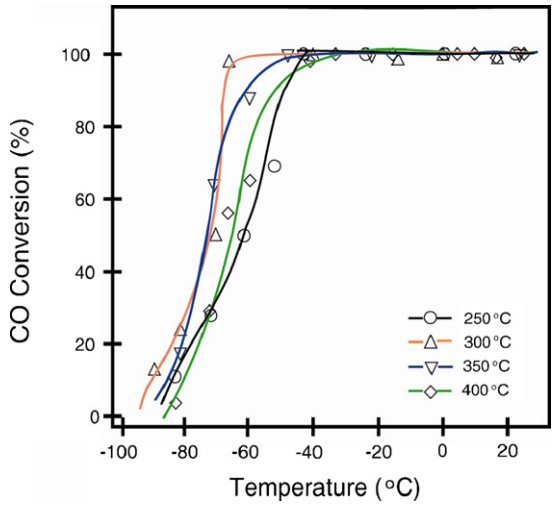

Fig. 9. Catalytic performances of Co_3O_4 catalysts calcined at different temperatures.

such a high activity. While in the present study, no preferred lattice plane exposure is needed for the low temperature CO conversion, this can be attributed to its appropriate surface properties such as Co^{3+}/Co^{2+} ratio and high surface area of the prepared materials.

4. Conclusion

Polycrystalline mesoporous Co_3O_4 has been successfully fabricated by a controlled thermal decomposition of micrometer-sized cobalt oxalate crystals. After calcined at given temperatures, the obtained nano-sized Co_3O_4 crystallites connected together to form mesoporous structure. Compared with the complicated grain-oriented growth of the highly catalytic active Co_3O_4 nanorods, this method is simple and efficient, and no grain orientation is needed. The mesoporous structure makes the Co3O4 nano-crystallites expose most active lattice planes on pore surface. The as-prepared material by calcination at 300 °C at a heating rate of 0.5 °C/min showed high catalytic activity for low temperature CO oxidation, and the full CO conversion can be achieved at as low as −70 °C.

Acknowledgements

This study was supported by National Nature Science Foundation of China, Grant no. 21073059, Program for Changjiang Scholars and Innovative Research Team in University (IRT0825) and the Fundamental Research Funds for the Central Universities no. WK1013001.

References

[1] M. Haruta, N. Yamada, T. Kobayashi, S. Iijima, J. Catal. 115 (1989) 301–309.
[2] M. Haruta, T. Kobayashi, H. Sano, N. Yamada, Chem. Lett. 16 (1987) 405–408.
[3] V. Idakiev, T. Tabakova, A. Naydenov, Z.Y. Yuan, B.L. Su, Appl. Catal. B: Environ. 63 (2006) 178–186.
[4] Y. Denkwitz, M. Makosch, J. Geserick, U. Hoermann, S. Selve, U. Kaiser, N. Huesing, R.J. Behm, Appl. Catal. B: Environ. 91 (2009) 470–480.
[5] T. Tabakova, G. Avgouropoulos, J. Papavasiliou, M. Manzoli, F. Boccuzzi, K. Tenchev, F. Vindigni, T. Ioannides, Appl. Catal. B: Environ. 101 (2011) 256–265.
[6] A. Stephen, K. Hashmi, G.J. Hutchings, Angew. Chem. Int. Ed. 45 (2006) 7896–7936.
[7] M. Comotti, W. Li, B. Spliethoff, F. Schűth, J. Am. Chem. Soc. 128 (2006) 917–924.
[8] D. Widmann, Y. Liu, F. Schűth, R.J. Behm, J. Catal. 279 (2010) 292–305.
[9] E.C. Njagi, C.-H. Chen, H. Genuino, H. Galindo, H. Huang, S.L. Suib, Appl. Catal. B: Environ. 99 (2010) 103–110.
[10] F. Grillo, M.M. Natile, A. Glisenti, Appl. Catal. B: Environ. 48 (2004) 267–274.
[11] Y. Yu, T. Takei, H. Ohashi, H. He, X. Zhang, M. Haruta, J. Catal. 267 (2009) 121–128.
[12] C. Xu, Y. Liu, C. Zhou, L. Wang, H. Geng, Y. Ding, ChemCatChem 3 (2011) 399–407.
[13] H. Tűysűz, M. Comotti, F. Schűth, Chem. Commun. 402 (2008) 2–4024.
[14] X. Xie, L. Li, Z.-Q. Liu, M. Haruta, W. Shen, Nature 458 (2009) 746–749.
[15] G. Marbán, I. López, T. Valdés-Solís, A.B. Fuertes, Int. J. Hydrogen Energy 33 (2008) 6687–6695.
[16] I. López, T. Valdés-Solís, G. Marbán, Chemcatchem 3 (2011) 734–740.
[17] C. Yu, L. Zhang, J. Shi, J. Zhao, J. Gao, D. Yan, Adv. Funct. Mater. 18 (2008) 1544–1554.
[18] C. Cong, T. Yi, J. Hong, H. Tao, K. Zhang, Chin. J. Inorg. Chem. 22 (2006) 379–383.
[19] G. Tyuliev, S. Angelov, Appl. Surf. Sci. 32 (1988) 381–391.
[20] P.G. Harrison, I.K. Ball, W. Daniell, P. Lukinskas, M. Cespedes, E.E. Miro, M.A. Ulla, Chem. Eng. J. 95 (2003) 47–55.
[21] N. Bahlawane, E.F. Rivera, K. Kohse-Hoinghaus, A. Brechling, U. Kleineberg, Appl. Catal. B: Environ. 53 (2004) 245–255.